

A case study of the fluid structure interaction of a Francis turbine

C Müller¹, T Staubli², R Baumann³ and E Casartelli²

¹Kraftwerke Oberhasli AG, 3862 Innertkirchen, Switzerland,

²HSLU T&A, Fluid Mechanics and Hydro Machines, Horw, Switzerland,

³HSLU T&A, Mechanical Systems, Horw, Switzerland,

e-mail: thomas.staubli@hslu.ch

Abstract: The Francis turbine runners of the Grimsel 2 pump storage power plant showed repeatedly cracks during the last decade. It is assumed that these cracks were caused by flow induced forces acting on blades and eventual resonant runner vibrations lead to high stresses in the blade root areas. The eigenfrequencies of the runner were simulated in water using acoustic elements and compared to experimental data. Unsteady blades pressure distribution determined by a transient CFD simulation of the turbine were coupled to a FEM simulation. The FEM simulation enabled analyzing the stresses in the runner and the eigenmodes of the runner vibrations. For a part-load operating point, transient CFD simulations of the entire turbine, including the spiral case, the runner and the draft tube were carried out. The most significant loads on the turbine runner resulted from the centrifugal forces and the fluid forces. Such forces effect temporally invariant runner blades loads, in contrast rotor stator interaction or draft tube instabilities induce pressure fluctuations which cause the temporally variable forces. The blades pressure distribution resulting from the flow simulation was coupled by unidirectional-harmonic FEM simulation. The dominant transient blade pressure distribution of the CFD simulation were Fourier transformed, and the static and harmonic portion assigned to the blade surfaces in the FEM model. The evaluation of the FEM simulation showed that the simulated part load operating point do not cause critical stress peaks in the crack zones. The pressure amplitudes and frequencies are very small and interact only locally with the runner blades. As the frequencies are far below the modal frequencies of the turbine runner, resonant vibrations obviously are not excited.

1. Introduction

Flow induced vibrations and noise observed in hydraulic machinery extent over several decades. An overview on some of typically observed phenomena is given by Dörfler et al. [1] in Figure 1. Frequencies emitted by the collapse of cavitation bubbles in machines were measured even in the MHz range, Zeqiri et al. [2]. On the lower end, if the entire hydraulic system is included, periods of oscillations of several minutes are experienced. Classifying phenomena into externally excited and self-excited effects rotor stator interaction and hydraulic unbalance belong to the first group, vortex shedding (von Karman vortex street), draft tube vortex rope, and rotating stall to the second group (Staubli [3]).

Object of investigation of the presented study were the Francis turbine runners of the pump storage plant of Grimsel 2, Switzerland, which showed during the last decades repeatedly cracks. Goal of the study was to identify or exclude sources of fluid loading and possible resonant response of the mechanical structure. The work presented here is an extract from the master thesis of Müller [5].



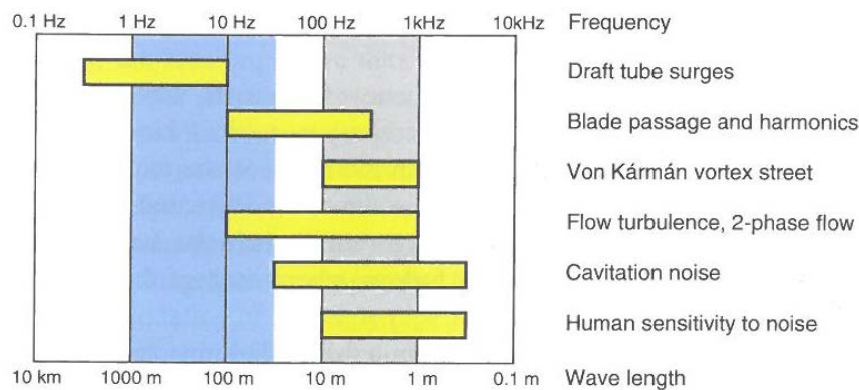


Figure 1. Typical frequency ranges and wave length observed in hydro machines. Dörfler *et al.* [1]

The combination of CFD- and FEM-simulations with the goal to analyze the rotor stator interactions has become the state-of-the-art. Pioneering work has been presented by Coutu *et al.* [6]. They computed the forced response computation of the runner structure under fluid loading due to flow and added mass effects. These procedures proved to be well suited for trouble shooting, especially in case of the occurrence of cracks, as was shown by Coutu *et al.* [7]

2. Analysis of the mode shapes in water

In a previous experimental study eigenfrequencies and associated mode shapes of the runner were determined based on dynamic impact tests. These tests were carried out in a pool with the runner suspended on a crane (Müller [5]), see Figure 2). Applying the same water body and boundary conditions for a FEM analysis the correctness of the simulated eigenfrequencies could be validated. In a second step the water body was simulated according to the turbine configuration, including approximated rotor side spaces. With this new water body lower eigenfrequencies were determined in the simulation (Müller [4]). This effect can be explained by the shorter distances to the system boundaries of the surrounding water, see Figure 3. In the experiment the influence of free surface lead to an increased dissipation in the experiment and to a reduction of the added mass effects.



Figure 2. Experimental modal analysis in water

The surrounding water volume was simulated as acoustic body. At the inlet and outlet radiation boundaries were chosen. The contact area between water and runner were modelled with the MPC-algorithm and the contact was chosen to be asymmetric. The fixation of the runner at the shaft was chosen to be zero-displacement.

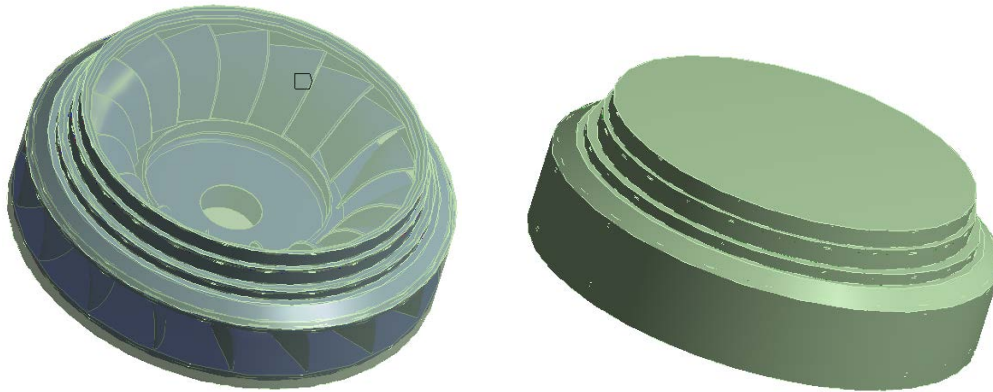


Figure 3. FEM-model of the runner (left, $6 \cdot 10^5$ elements) and model of the surrounding water (right, $1.6 \cdot 10^6$ elements)

	mode shape diameter (m/n), referenced to the hub outer diameter	view from hub side	view from shroud side	comparative stress (von Mises) view from shroud side Location of maximum stress is marked in red TS=hub und K=shroud (has only qualitative meaning)
a	1. bending mode (ND=1) f = 219 Hz = 0.36 f in air			 TS
b	2. bending mode (ND=2) f = 241 Hz = 0.35 f in air			 TS

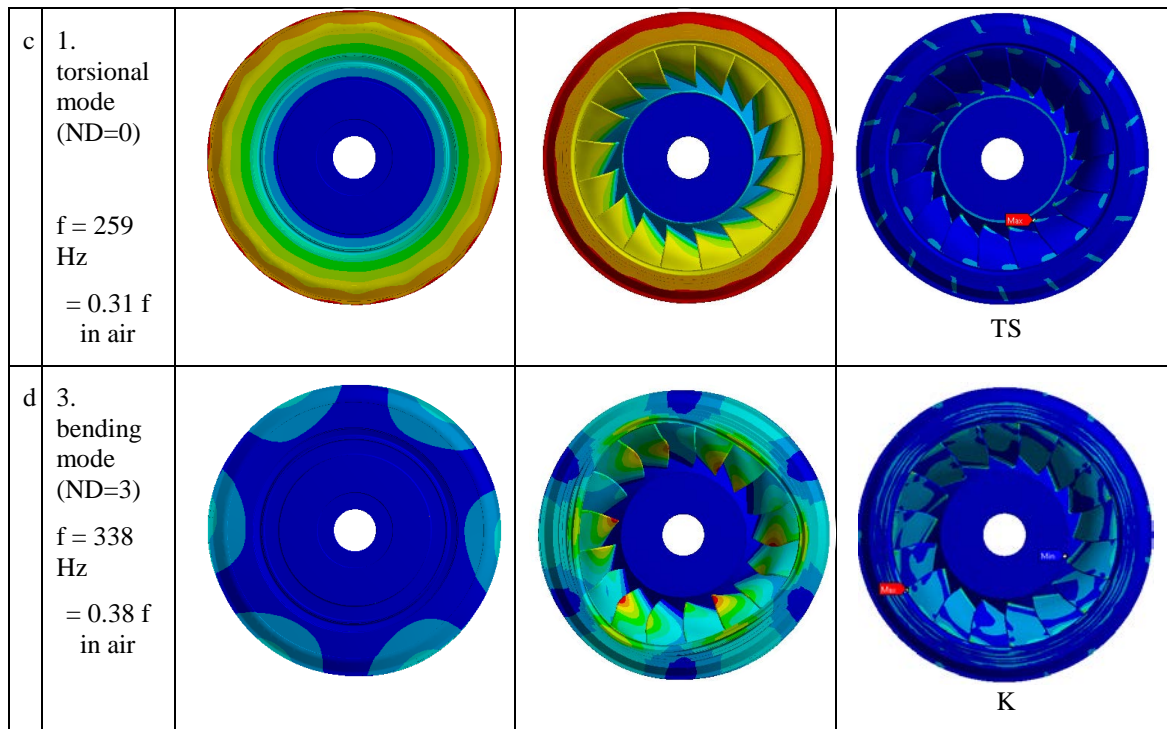


Figure 4. The first 4 modes of vibration of the runner in water resulting from modal analysis with FEM (blue = no deformation)

3. Rotor stator interaction (RSI) and condition of existence of excitation

Basic RSI frequencies are excited by the number of runner and guide vanes multiplied with the speed of rotation. Frequencies of 212.5 Hz and 300 Hz result from the given 17 runner and 24 guide vanes and a speed of rotation of 12.5 Hz.

Dubas [8] deduced that in addition to resonance condition with exciting frequencies equal to eigenfrequency also a condition of existence must be fulfilled.

This condition of existence can be formulated as:

$$mz_1 \pm ND = m'z_0$$

with z_1 = number of guide vanes, z_0 = number of runner blades, ND = nodal diameter, m, m' = integer, multiple of $z_{0,1}$

The RSI excitation frequency f_e is calculated taking the condition of existence into account as:

$$f_e = (mz_1 \pm ND)f_0 = m'z_0 f_0$$

with $f_0 = 12.5$ Hz

The values marked in red in Table 1 correspond to node diameters below ND = 10. The associated excitation frequencies lie between 300 and 2100 Hz. The essential question is whether these frequencies calculated on the basis of the runner speed and the number of guide vanes and runner blades will excite one of the determined eigenfrequencies of the runner. A comparison with the simulated eigenfrequencies shows that such a resonance can be excluded, since there is no agreement with the theoretically determined excitation frequencies.

Table 1. Theoretical possible mode excitation (marked in red) for a rotational frequency of $f_0 = 12.5$ Hz

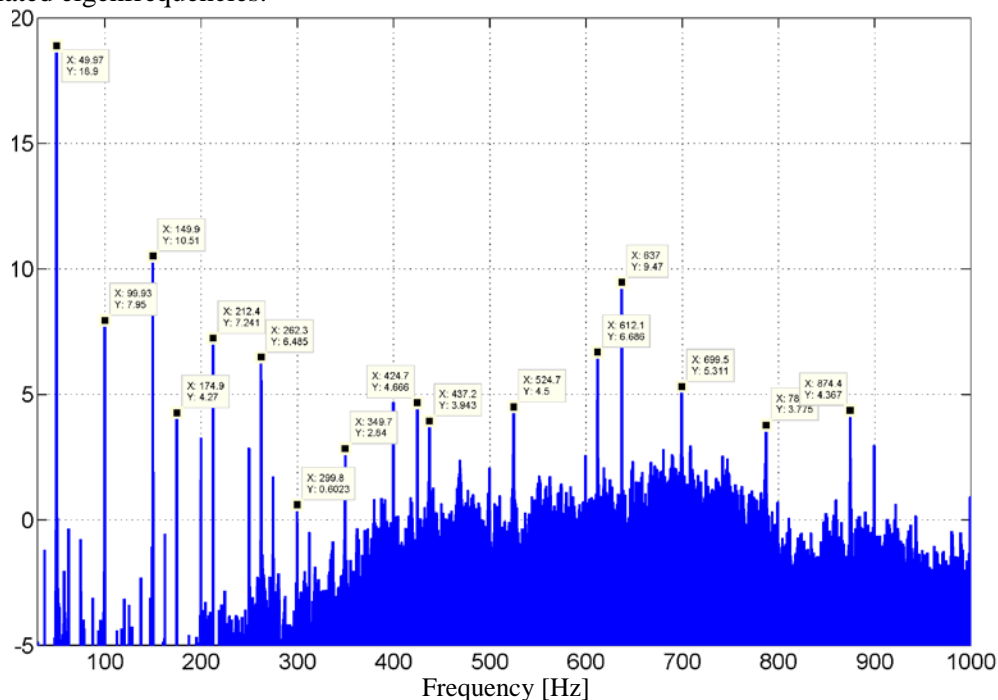
fe [Hz]	m [-]		1	2	3	4	5	6	7	8	9	10
	m' [-]	m [-]										
300	1		7	10	27	44	61	78	95	112	129	146
600	2		31	14	3	20	37	54	71	88	105	122
900	3		55	38	21	4	13	30	47	64	81	98
1200	4		79	62	45	28	11	6	23	40	57	74
1500	5		103	86	69	52	35	18	1	16	33	50
1800	6		127	110	93	76	59	42	25	8	9	26
2100	7		151	134	117	100	83	66	49	32	15	2
2400	8		175	158	141	124	107	90	73	56	39	22
2700	9		199	182	165	148	131	114	97	80	63	46
3000	10		223	206	189	172	155	138	121	104	87	70

4. Measured excitation

The measurements of noise intensity and the associated spectra provide a good indication of frequencies of pressure pulsations being existent in the flow, transferred to the casing and then radiated as noise, as well as for resonant vibrations of mechanical structures within the measured frequency range. Such spectra were measured for continuous operation at part and full load as well as for transient start up operation. All measurements were performed using a commercial microphone and standard spectrum analysis software.

The maximum peaks found in the spectra were at 50Hz and higher harmonics. This frequency corresponds to the grid frequency and was considered to be neither an exciting nor resonant frequency.

Prominent peaks were also observed at 212.5Hz and 300Hz in all measured spectra corresponding to the RSI excitation frequencies. Other frequencies repeating in all spectra were at 263 Hz, 350 Hz, 437 Hz, 526 Hz and 612Hz (Figure 5). All these frequencies are close to the simulated eigenfrequencies.

**Figure 5.** Spectrum of noise intensity (dBA) measured at 750 rpm and guide vane opening

from 16.4° to 25.5°, power from 51 MW to 85.4 MW, flow rate from 18.1 m³/s to 26.5 m³/s.

5. CFD simulation

In a series of internal reports of the power plant operator noise and vibration were reported especially at part load operation with guide vane opening angles of less than 13°. For this reason a part load operating point was chosen in the presented study to investigate fluid loading and eventual resonance phenomena.

CFD simulations were carried out with ANSYS CFX 14.5. The simulation domain from inlet to outlet is displayed in Figure 6. Not simulated were the rotor side spaces and the labyrinth seals. The leakage, however, was calculated separately and the leakage flow was introduced. All key numbers describing the simulation are listed in Table 2.

Table 2. Key numbers of the mesh and its quality criteria, the solver, and convergence.

components	stationary domain: spiral with 24 stay vanes and 24 guide vanes, draft tube rotating domain: runner, hub and shroud cover, 17 vanes				
mesh	hexaeder (18 10 ⁶ elements), tetraeder (2 10 ⁵ elements) runner: 1.7 10 ⁶ elements spiral: 15.3 10 ⁶ elements draft tube: 1.2 10 ⁶ elements				
mesh quality	orth. Angle	exp. fac.	asp. rat.	y+	location
spiral	2.5	304·822	1710 (only locally)	<600 (only locally)	transition tongue-casing
runner	42.2	8	961	<123	
draft tube	22.3	86	1720 (only locally)	<460 (only locally)	support pipes of vortex stabilizer
type of analyses	transient with transient initial solution (5 revolutions) time step 0.00022 s (1_revolution), totally 2x5 revolutions (0.8 s).				
interfaces	spiral - runner and runner - draft tube: transient rotor-stator, no pitch change, GGI				
fluid	water, incompr. at 5_C				
boundary conditions	inlet: mass flow rate: 10.1 m ³ /s outlet: time averaged static pressure: 0 Pa reference pressure: 0 Pa				
solver	advection scheme: high res. transient scheme: second order backward Euler convergence control: 1-10 inner loops, res. target: 1e-5				
turbulence model	SST				
convergence	RMS res. mom < 5e-6, RMS res max < 1e-2, imbalance < 1e-4				
hardware	parallel simulation on a cluster with 36 bis 72 CPUs, single precision				

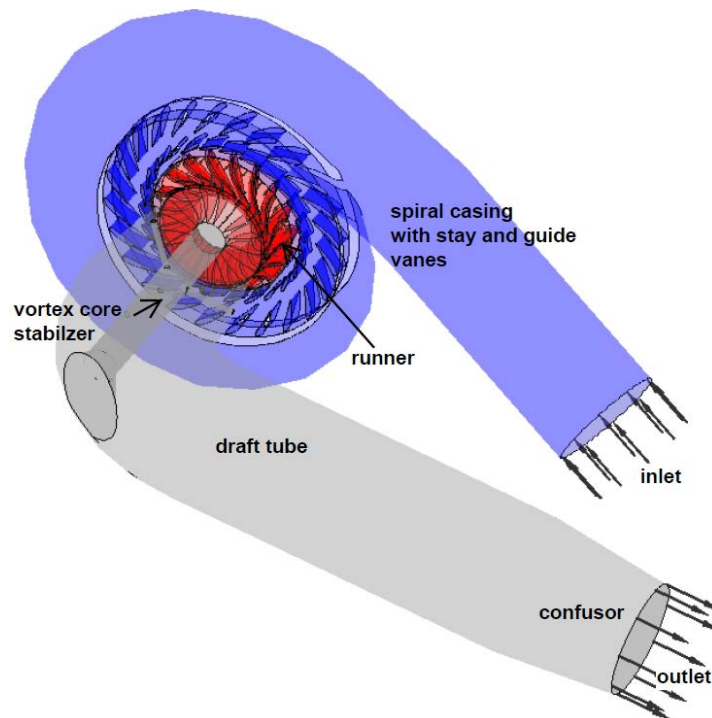


Figure 6. Simulation domain with spiral casing, runner, stay and guide vanes, and draft tube.

The flow fields at part load operation were analysed in detail. A typical spectrum of the pressure fluctuation in the vaneless space between guide vanes and runner is given in Figure 7. The largest peak results from the RSI frequency of 212.5 Hz. The frequencies at the very low end of the spectrum result from the vortex formation in the draft tube see Figure 8.

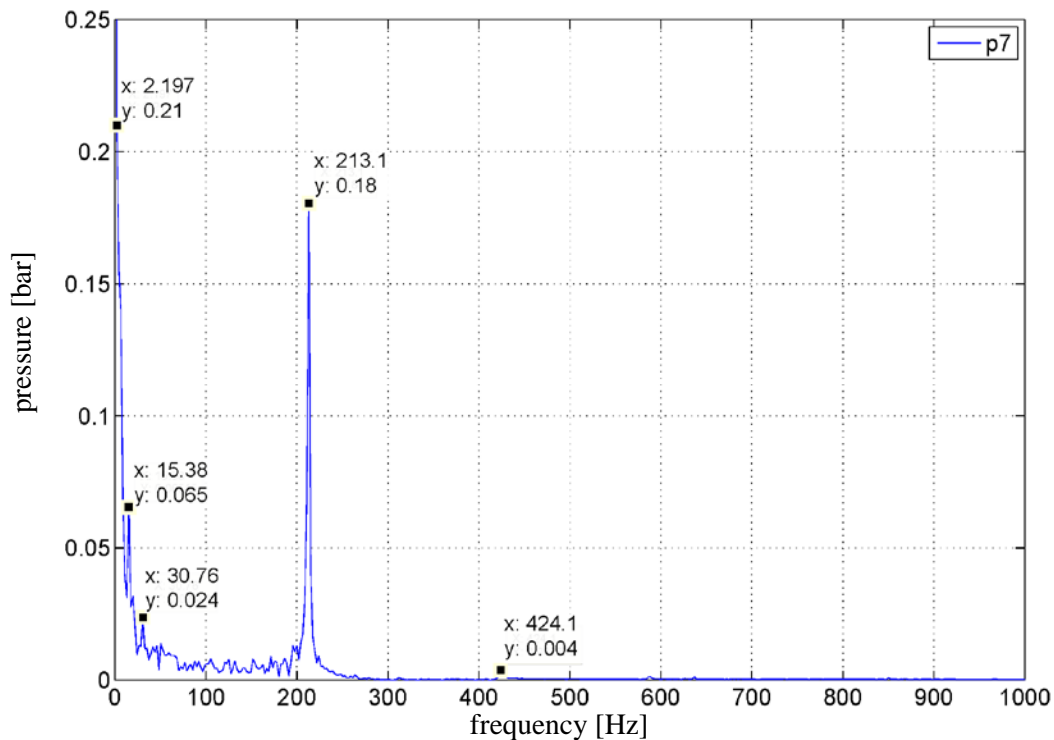


Figure 7. Spectrum of pressure fluctuations in the vaneless space obtained from CFD.

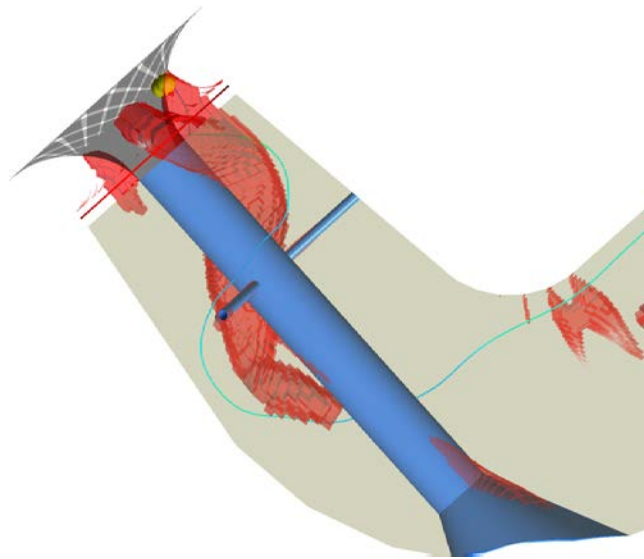


Figure 8. Simulated vortex rope at the investigated part load operation.

6. Unidirectional coupling of CFD simulation and FEM model

The method of unidirectional harmonic load transfer can be applied if the mechanical deformation resulting from the fluid loading is small, what can be assumed for the present study. The advantage of the unidirectional coupling is the considerable reduction of computational time. Attempts of bi-directional coupling failed after a rotation of 45° due to excessive RAM demand. Disadvantage of the unidirectional harmonic coupling is that excitation by stochastic pressure fluctuations are not taken into account. The individual steps, which have to be followed during this procedure, are described in Figure 9.

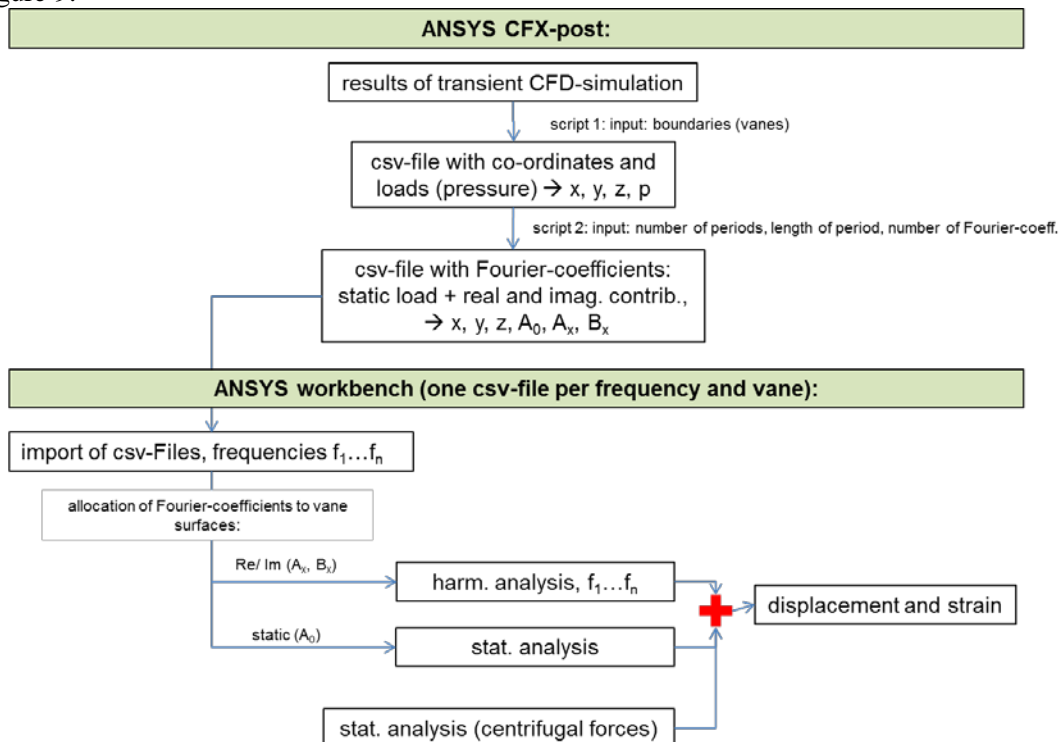


Figure 9. Flow chart of a unidirectional, harmonic coupling with ANSYS Workbench.

7. Results

From superposition of deformation and stress resulting from the harmonic analysis at the various frequencies, with the ones resulting of the static loads and centrifugal forces, it becomes possible to determine the total deformation and the total stress, Figure 10.

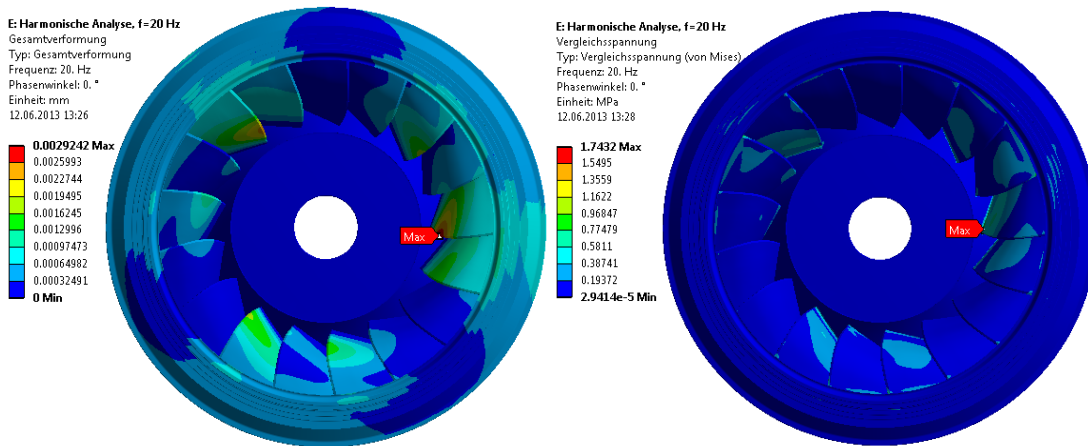


Figure 10. Total deformation (left) and von Mises stress (right) for f= 20Hz.

In most cases maximum stress was predicted at the location where cracks occurred, however, the predicted amplitudes were by an order of magnitude too small to be the reason of the runner damages. The highest stress values evaluated by the harmonic analysis are caused by the unstable draft tube flow and reach up to 1.74 MPa at the crack location. Superimposing to these stresses the stresses provoked by the static loading (51.6 MPa) and the centrifugal forces (95.9 MPa) a resulting stress of 91.8 MPa is calculated.

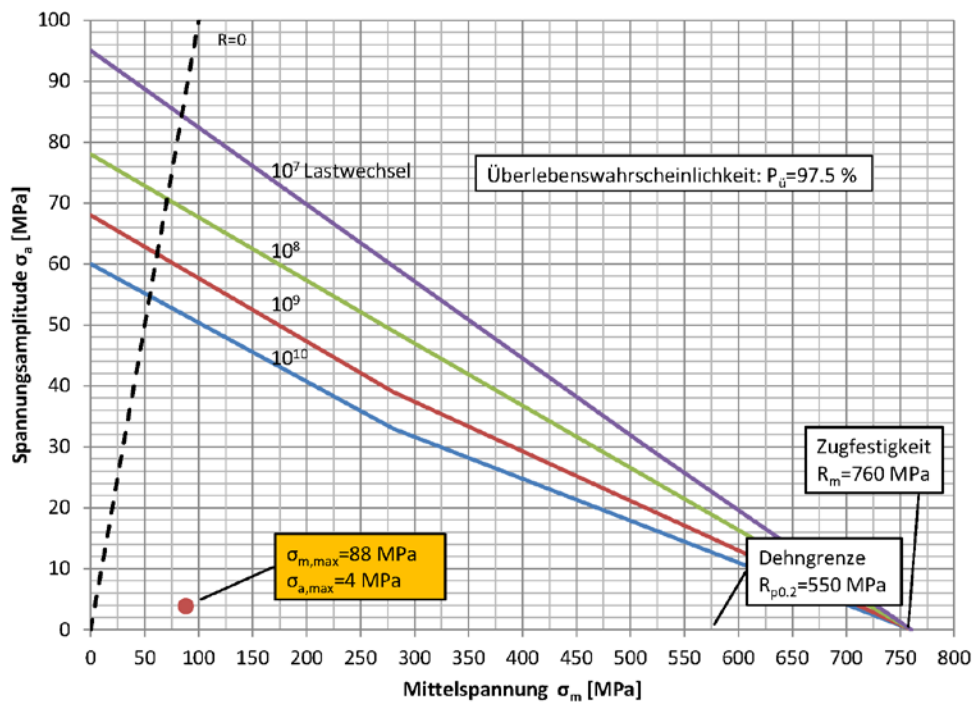


Figure 11. Haigh diagram of G-X5 Cr Ni 13 4 with the calculated stresses of the part load operating point.

With the determined static and dynamic stresses a life cycle analysis can be performed. From the Haigh diagram displayed in Figure 11 can be concluded that, with the prevailing number of stress cycles of about $4 \cdot 10^{10}$ and an assumed constant operation at the investigated part load operation, fatigue will not yet lead to cracks. However, since this life cycle investigation did not include the entire field of operation, not all starts and stops, consolidated statements are not possible.

8. Conclusions

Observed noise phenomena can be associated with the vortex rope prediction, which was found in the CFD simulation. Such a part load rope will cavitate and cause noise and vibrations, a subject which has not been addressed. These pulsations should be further investigated in order to clarify if this might be the reason for the cracks.

Also the location of highest stress predicted in the simulation agrees well with the location of the observed cracks. However, the amplitudes of the predicted local stresses do, by far, not allow the conclusion that the cracks are caused by the part load fluid structure interaction. It was also not possible to relate a certain mode shape of the natural vibration to the crack formation.

References

- [1] Dörfer P, Sick M and Coutu A 2012 Flow-induced pulsation and vibration *Hydroelectric Machinery* (Springer, Zurich)
- [2] Zeqiri B, Lee N D, Hodnett M and Gela P N 2003 A novel sensor for monitoring acoustic cavitation. Part II: prototype performance *IEEE Transactions on Ultrasonics, Ferroelectrics, and Frequency Control* **50**(10)
- [3] Staubli T 1993 Einfluss vom umgebenden fluid auf das Schwingungsverhalten von Strömungsmaschinen *VDI-Berichte*
- [4] Müller C 2013 Modalanalysen an einem Francis-Turbinenlaufrad *MSE-thesis, Hochschule Luzern Technik & Architektur*
- [5] Müller C 2013 FSI and einem Francisturbinenlaufrad *MSE-Vertiefungsmodul, Hochschule Luzern Technik & Architektur*
- [6] Coutu A, Aunemo H, Badding B and Velagandul O 2005 Dynamic Behavior of High Head Francis Turbine *Hydro Villach* 17-20
- [7] Coutu A, Roy M D, Monette C and Nennemann B, 2008 Experience with rotor-stator interactions in high head Francis runner *24th IAHR Symposium on Hydraulic Machinery and Systems* (Foz do Iguassu, Brazil)
- [8] Dubas M 1984 Über die Erregung infolge der Periodizität von Turbomaschinen *Ingenieur-Archiv* (Springer-Verlag, Zürich) **54** 413-426
- [9] Krishnamachar P, Fay A and Rangnekar S 2008 Runner core cavitation near full load in Francis turbines *Water Power Magazine* [Version June 2013]
- [10] Torklep A M 2012 Pressure oscillations during start and stop of a high head Francis turbine master thesis, *Norwegian University of Science and Technology* (Trondheim)